Journal of Cotton Research

RESEARCH

Open Access

Effects of mepiquat chloride and plant population density on leaf photosynthesis and carbohydrate metabolism in upland cotton

LUO Haihua[1,2], ZHANG Zhengxian[1], WU Jianfei[1], WU Zhenjiang[2], WEN Tianwang[1*] and TANG Feiyu[1*]

Abstract

Background Mepiquat chloride (MC) application and plant population density (PPD) increasing are required for modern cotton production. However, their interactive effects on leaf physiology and carbohydrate metabolism remain obscure. This study aimed to examine whether and how MC and PPD affect the leaf morpho-physiological characteristics, and thus final cotton yield. PPD of three levels (D1: 2.25 plants·m^{-2}, D2: 4.5 plants·m^{-2}, and D3: 6.75 plants·m^{-2}) and MC dosage of two levels (MC0: 0 g·ha^{-2}, MC1: 82.5 g·ha^{-2}) were combined to create six treatments. The dynamics of nonstructual carbohydrate concentration, carbon metabolism-related enzyme activity, and photosynthetic attributes in cotton leaves were examined during reproductive growth in 2019 and 2020.

Results Among six treatments, the high PPD of 6.75 plants·m^{-2} combined with MC application (MC1D3) exhibited the greatest seed cotton yield and biological yield. The sucrose, hexose, starch, and total nonstructural carbohydrate (TNC) concentrations peaked at the first flowering (FF) stage and then declined to a minimum at the first boll opening (FBO) stage. Compared with other treatments, MC1D3 improved starch and TNC concentration by 5.4%~88.4%, 7.8%~52.0% in 2019, and by 14.6%~55.9%, 13.5%~39.7% in 2020 at the FF stage, respectively. Additionally, MC1D3 produced higher transformation rates of starch and TNC from the FF to FBO stages, indicating greater carbon production and utilization efficiency. MC1D3 displayed the maximal specific leaf weight (SLW) at the FBO stage, and the highest chlorophyll a (Chl a), Chl b, and Chl a + b concentration at the mid-late growth phase in both years. The Rubisco activity with MC1D3 was 2.6%~53.2% higher at the flowering and boll setting stages in both years, and 2.4%~52.7% higher at the FBO stage in 2020 than those in other treatments. These results provided a explanation of higher leaf senescence-resistant ability in MC1D3.

Conclusion Increasing PPD coupled with MC application improves cotton yield by enhancing leaf carbohydrate production and utilization efficiency and delaying leaf senescence.

Keywords *Gossypium hirsutum* L., Mepiquat chloride, Plant population density, Carbohydrate metabolism, Photosynthesis

*Correspondence:
Wen Tianwang
wentianwangjxau@163.com
Tang Feiyu
fytangcau@163.com
[1] Key Laboratory of Crop Physiology, Ecology and Genetic Breeding, Ministry of Education, College of Agronomy, Jiangxi Agricultural University, Nanchang 330045, China
[2] Jiangxi Institute for Industrial Crops Research, Jiujiang 332005, China

Introduction

Upland cotton (*Gossypium hirsutum* L.) is a leading fiber crop worldwide with an indeterminate growth habit. Modern crop production requires high plant population density (PPD) and compact plant architecture (Mao et al. 2014). Cotton plants tend to produce excessive vegetative growth when grown in a fertile, well-irrigated, and suitable environment (Reddy et al. 1990, 1992), which leads to increased population shading (Mao et al. 2014). Mepiquat chloride (N, N-dimethylpiperidinium, MC) and PPD are two common agronomic practices to manage cotton growth. They are commonly used to create compact plants with short limbs conducive to mechanical harvest (Nichols et al. 2003; Wilson et al. 2007; Mao et al. 2014).

MC is a gibberellin biosynthesis inhibitor (Rademacher 2000), which is widely utilized for controlling excessive vegetative growth, such as the reduction of plant height, leaf area, the number of main-stem nodes, and internode length, thus resulting in more compact plant stature (Reddy et al. 1990, 1992; Gu et al. 2014). Other physiological responses to MC application include that the contents of leaf chlorophyll, soluble sugar, and starch were enhanced (Reddy et al. 1996; Zhao and Oosterhuis 2000; Tung et al. 2018a), and promoted early maturity (York 1983; Owen Gwathmey and Chism Craig 2003; Pettigrew and Johnson 2005). The effects of MC on photosynthesis and yield have been inconsistent among previous studies. Reddy et al. (1996) reported that net photosynthetic rate decreased by 25% in MC-treated leaves, and in another experiment Reddy et al. reported (1995) that net photosynthetic rate reduced by 30% due to the application of 30 $\mu g \cdot g^{-1}$ MC. Tung et al. (2018a) found that photosynthesis reduced by 1%～28% with increasing MC dosage. Conversely, Zhao and Oosterhuis (2000) observed that MC application improved leaf CO_2 exchange rate. Hodges et al. (1991) reported that MC increased the canopy gross photosynthesis on the second day post foliar MC spray. Yield response to MC has been erratic, ranging from positive (York 1983; Cathey and Meredith 1988; Biles and Cothren 2001; Nichols et al. 2003; Siebert and Stewart 2006; Mao et al. 2015; Zhao et al. 2017; Shi et al. 2022) to negative (York 1983; Cathey and Meredith 1988; Ren et al. 2013; Tung et al. 2018a, b) to none (Pettigrew and Johnson 2005). The cotton yield response largely depends on the rate and timing of MC application (Reddy et al. 1995), environmental factors, moisture and fertilizer availability (Reddy et al. 1992), planting date (Cathey and Meredith 1988; Pettigrew and Johnson 2005), planting density, and cultivar (Zhao et al. 2017). Biles and Cothren (2001) reported that multiple, lower-dosage MC applications produced higher cotton yield than a single application at the early bloom stage. In most cases, MC decreases boll density and lint percentage but increases boll and seed weights (York 1983; Ren et al. 2013; Mao et al. 2015; Shi et al. 2022). The decreased lint percentage is attributed to the enhanced seed weight (York 1983), while the increased boll weight is partly due to the appropriate distribution of harvestable bolls mostly located at the inner fruiting positions on the middle-lower sympodia (Mao et al. 2015).

PPD effects on cotton growth and yield have been investigated extensively in past decades (Galanopoulou-Sendouka et al. 1980; Bednarz et al. 2005; Dong et al. 2006; O'Berry et al. 2008; Wrather et al. 2008; Khan et al. 2017; Shah et al. 2017). Cotton yield remains stable across a wide range of plant densities of 3.3 to 10.5 $plants \cdot m^{-2}$ through the manipulation of either yield components (boll density and boll weight) or dry matter accumulation and partitioning (Dai et al. 2015). Enhancing PPD typically increases boll density but decreases boll weight, and lint percentage is little affected (Bednarz et al. 2005; Dong et al. 2006, 2012; Dai et al. 2015). Leaf senescence is delayed through increasing PPD (Dong et al. 2012; Dai et al. 2015; Luo et al. 2018). High PPD under deficit irrigation can achieve a comparable yield to medium PPD under regular irrigation through increasing plant biomass and harvest index (Zhang et al. 2016). The late-planted cotton with higher PPD produced a yield equal to the early-planted cotton with lower PPD (Dong et al. 2006). High PPD can reduce the nitrogen rate by 20%～30% from the traditionally recommended rate without compromising cotton yield, which is probably attributed to the delayed leaf senescence and enhanced N use efficiency (Luo et al. 2018).

High PPD coupled with the optimal timing and dosage of MC improves cotton productivity (Ren et al. 2013; Gu et al. 2014; Chen et al. 2021). High PPD tends to concentrate boll setting on first-position sympodial sites (Wilson et al. 2007). Combined high PPD and MC application produce more bolls residing on lower (Gwathmey and Clement 2010) or low-middle sympodia (Mao et al. 2015), while Chen et al. (2021) reported more bolls were at the upper and middle canopy. More concentrated boll distribution due to the combination of high PPD and MC application implies a more synchronous demand for carbohydrates (Gwathmey and Clement 2010). Therefore, leaf photosynthesis and carbohydrate dynamics in the compact, high-density cotton population are expected to be different from normal cotton populations. However, limited information is available on PPD and MC application effects on cotton leaf photosynthetic production. Tung et al. (2018a) reported the effects of MC application on leaf photosynthesis and carbohydrate metabolism in a short-season cotton production system which was characterized by late sowing, high planting density, and single fertilization. Nevertheless, the interactive effects of PPD and MC application on cotton growth and yield are lacking for full-season cotton under optimal planting. PPD and MC have been hypothesized to affect cotton yield through the regulation of leaf physiology (mainly photosynthesis-related) and carbon metabolism. To test the hypothesis, three levels of PPD (low, middle, high) and two dosages of MC application (MC free and MC application) were combined to create six cotton populations with different leaf morpho-physiological traits. The objectives of this study were to: i) examine PPD and MC application effects on cotton yield, yield components, biological yield, and harvest index; ii) explore the effects of PPD and MC application on leaf morphological and photosynthetic traits, including specific leaf weight (SLW), chlorophyll content, net photosynthetic rate (*P*n); iii) determine the dynamics of nonstructural carbohydrate concentration and carbon metabolism enzyme activity in response to PPD and MC application.

Materials and methods

Experimental design

A mid-maturation upland cotton line 4003–6 was field-grown at the experimental station of Jiangxi Institute for Industrial Crops Research, Jiujiang, China (29°42'N, 115°50'E) in 2019 and 2020. The soil type was tidal sand soil, with a neutral pH of 7.4. The upper 20 cm soil layer contained 18.6 $g·kg^{-1}$ of organic matter, 1.16 $g·kg^{-1}$ of total N, 1.04 $g·kg^{-1}$ of total P, 16.7 $g·kg^{-1}$ of total K, 74.5 $mg·kg^{-1}$ of available N, 34.2 $mg·kg^{-1}$ of available P, and 327 $mg·kg^{-1}$ of available K. Direct seeding was adopted in 2019 and shifted to seedling transplanting in 2020 due to the full standing availability of the latter. The planting dates were May 6, 2019, and April 10, 2020, and the transplanting date was May 10, 2020. The experiment was designed as a split-split plot design with three replications, with the whole plot assigned to years, the split-plot to MC dosage, and the split-split plot to PPD. Each plot consisted of eight rows of cotton with 6.24 m in length and 9.12 m in width. The row spacing was 1.12 m. The MC application included two levels of dosage (MC0: 0 $g·ha^{-1}$, MC1: 82.5 $g·ha^{-1}$), conforming to a local conventional MC schedule. The application dosages were 7.5 $g·ha^{-1}$ at 57 and 67 days post sowing (DPS), 30 $g·ha^{-1}$ at 81 and 91 DPS, and 45 $g·ha^{-1}$ at 101 and 111 DPS in 2019 and 2020, respectively. A foliar spray of pure water served as the control. PPD was classed into three levels (D1: 2.25 $plants·m^{-2}$, D2: 4.5 $plants·m^{-2}$, and D3: 6.75 $plants·m^{-2}$). The PPD gradient was designed given the local PPD recommendation of 3.75 to 4.5 $plants·m^{-2}$ for the conventional (non-hybrid) cotton in the Yangtze River valley region, China (Dong 2013). The interplant distance was 39.0 cm at D1, 19.5 cm at D2, and 13.0 cm at D3. Composite fertilizer 19–19-19 (19% NH_4^+-N, 19% phosphorus, and 19% potassium oxide) was incorporated into soils at the peak squaring (PS) stage at a rate of 225 $kg·ha^{-1}$, and flowering to boll setting (FB) stage at a rate of 600 $kg·ha^{-1}$ in 2019 and 2020.

Sampling procedure and data collection

Four samplings were taken and adjusted to the phenological characteristics at PS (64 DPS in 2019 and 75 DPS in 2020), the first flowering (FF; 71 DPS in 2019 and 83 DPS in 2020), FB (89 DPS in 2019 and 107 DPS in 2020), and the first boll opening (FBO; 117 DPS in 2019 and 125 DPS in 2020). Within a plot, selected plants were spaced far away from each other to ensure the growth of the remaining plants was not influenced by the earlier sampling of other plants. Four individual plants in each of the plots were uprooted and washed free of soil and then immediately divided into five parts: root, main stem, branch (petiole), leaf blade, and reproductive parts. All green leaves of each sample were scanned by a scanner (Epson Expression 12000XL), and the resulting images were translated into real leaf areas using image analysis software (Image J). Afterward, those leaves were oven-dried at 105 °C for 0.5 h and then at 60 °C until constant weights were achieved and then weighed. The SLW was calculated by the leaf biomass divided by the corresponding leaf area. In addition, the fourth main-stem leaf from the apex was sampled separately from each plot for analysis of physiological parameters. Cotton yield and its components were determined as described by Tang and Luo (2023). The biological yield was obtained by summing the dry weight of all plant parts at the maturity stage, and the harvest index was defined as the seed cotton yield to the biological yield ratio.

Net photosynthetic rate (*P*n) and SPAD value

*P*n was measured on the youngest fully expanded, healthy, and fully sunlit leaves, typically the fourth leaf from the apex using a portable photosynthesis system (L1-6400, Li-Cor, Lincoln, NE, USA) at early flowering (EF; 80 DPS in both years) and FB (103 DPS in both years), respectively. All measurements were taken between 9:00 and 11:00 on cloudless days with the photosynthetic photon flux density exceeding 1 500 $μmol·m^{-2}·s^{-1}$. SPAD values were read by a SPAD meter (SPAD 502 Plus, Konica Minolta, Japan) at the same time. Four plants in each plot were examined and the mean values were calculated.

Chlorophyll concentration

Chlorophyll (Chl) concentrations were determined as described by Li (2000) with minor modifications. Briefly, 0.1 g of fresh leaves was placed in a 2.5 mL centrifuge tube that contained a steel ball of 2 mm in diameter. After the addition of 1 mL pre-chilled ethanol (95%, v/v), the tissues were homogenized at 60 Hz for 30 s in a low-temperature grind miller (N9548, Hoder, Beijing, China) and repeated four times in a total of 2 min. The homogenate was transferred into a centrifuge tube and diluted to 10 mL with 95% ethanol, where the extraction was performed for 12 h under the condition of shade. The chlorophyll concentration in the supernatant was spectrophotometrically determined by measuring the absorbance at 665 nm and 649 nm for Chl a and Chl b. The formulas for the calculation of chlorophyll concentration were as follows: Chl a = $13.95*A_{665} - 6.88*A_{649}$; Chl b = $24.96*A_{649} - 7.32*A_{665}$.

Carbohydrate analysis

Nonstructural carbohydrates, such as glucose, fructose, sucrose, and starch, were extracted and quantified following previous procedures (Luo et al. 2019; Chen et al. 2020). Total nonstructural carbohydrate (TNC) concentration was defined as the sum of glucose, fructose, sucrose, and starch concentration.

Enzyme extraction and assay

About 0.1 g of fresh leaves were put into a 2.5 mL liquid nitrogen-frozen centrifuge tube which contained a steel ball of 2 mm in diameter. After the addition of 1 mL pre-cooled extraction buffer (50 mmol·L^{-1} Hepes–NaOH (pH 7.5), 2 mmol·L^{-1} Na_2-EDTA, 2.5 mmol·L^{-1} dithiothreitol (DTT), 10 mmol·L^{-1} $MgCl_2$, 0.05% Triton X-100, 1% (w/v) insoluble polyvinylpyrrolidone (PVP), 10% glycerol, and 0.3% (v/v) β-mercaptoethanol), the tissues were homogenized at 60 Hz for 30 s in a low-temperature grind miller (N9548, Hoder, Beijing, China) and repeated four times in a total of 2 min. Afterward, the homogenate was incubated for 1 h at a low temperature provided by ice. Vortexing was conducted at 10-min intervals, then centrifugated for 5 min at 12 000 r·min^{-1}. The supernatants were used in sucrose synthase (SuSy) and sucrose phosphate synthase (SPS) activity assays.

SPS activity was measured as reported by Luo et al. (2019) and Chen et al. (2020) with minor modifications. Briefly, each reaction contained 20 µL buffer solution which contained 50 mmol·L^{-1} Tris–Hcl (pH 7.0), 10 mmol·L^{-1} $MgCl_2$, 20 mmol·L^{-1} Glu-6-P, 20 mmol·L^{-1} Fru-6-P, 20 µL of 10 mmol·L^{-1} UDP-Glu, and 50 µL of extract in a total volume of 90 µL. The reaction was started by the addition of the extract, incubated at 30 °C for 10 min, and terminated with the addition of 200 µL of 2 mol·L^{-1} NaOH and 10 min of heating at 100 °C to destroy untreated hexose and hexose phosphate. After the solution was cooled to room temperature, 1.4 mL of 30% (w/v) HCl and 0.4 mL of 0.1% (w/v) resorcinol were added and the reaction was incubated at 80 °C for 10 min. After cooling to room temperature, sucrose concentration was calculated from a standard curve measured at 480 nm. SuSy was assayed as above but with 20 mmol·L^{-1} fructose substituting for Fru-6-P.

The activities of Ribulose bisphosphate carboxylase oxygenase (Rubisco) and Fructose-1, 6-bisphosphatase (FBPase) were measured following the procedures described in the manufacturer's guideline of assay kits (Suzhou Comin Biotechnology Co. Ltd, Suzhou, China).

Data analysis

Treatment effects on cotton yield, biological yield, harvest index, *P*n, and SPAD value were subjected to Analysis of Variance (ANOVA) using the General Linear Model procedure (GLM) in SPSS 18.0 software (Chicago, IL, USA). In the statistical analysis, MC, PPD, and year served as fixed effects and block (replicate) as a random factor. The PPD was nested within MC, which was nested within the year. For the ANOVA involved in SLW, chlorophyll concentration, nonstructural carbohydrate concentration, and carbon metabolism enzyme activity, MC, PPD, and sampling time served as fixed effects and block (replicate) as a random factor. The sampling time was nested with the PPD, while the latter was nested within the MC. The means were separated using Duncan's multiple range tests at $P \leq 0.05$. For parameters where year interacted with treatments were detected, the results were presented by years. Conversely, when statistically significant interaction with the year was not identified, treatment means were averaged across years. The figures were produced using Origin 8.5 and Origin 2021b.

To evaluate the utilization efficiency of nonstructural carbohydrates in cotton leaves over reproductive growth, the notion of transformation rate (TR) was introduced. Given a specific nonstructural carbohydrate component, it can be expressed as the following formula: TR (%) = (maximum concentration − minimum concentration) / maximum concentration × 100 (Shu et al. 2009; Tang et al. 2014).

Results

Seed cotton yield, biological yield, and harvest index

Year effects significantly affected seed cotton yield, biological yield, and harvest index (Supplementary Table S1). The PPD effect was significant for all traits. The MC effect was significant for biological yield and harvest index. The PPD by MC interaction exhibited significant effects on seed cotton yield and biological yield. The MC application decreased the biological yield, but increased the harvest index, thus remaining the seed cotton yield equivalent to the MC-free control (Table 1). At the given PPD range, biological yield was increased, but the harvest index decreased with increasing PPD. Among the six combinations of PPD and MC, MC1D3 (the combination of the MC application and the PPD of 6.75 plants·m^{-2}) exhibited the maximal seed cotton yield, and the biological yield followed by MC0D3, while MC1D1 possessed

Table 1 Effects of the mepiquat chloride and planting density on the seed cotton yield, biological yield, and harvest index in 2019 and 2020

Treatment	Seed cotton yield / ($kg \cdot ha^{-1}$)	Biological yield / ($kg \cdot ha^{-1}$)		Harvest index	
MC1D1	3 266.3e	6 708.4e		0.49a	
MC1D2	3 976.9c	8 725.2c		0.46bc	
MC1D3	4 518.0a	11 119.3a		0.41d	
MC0D1	3 562.0d	7 546.0d		0.47ab	
MC0D2	4 184.4b	9 453.9b		0.44c	
MC0D3	4 242.1b	10 915.6a		0.39e	
MC1	3 920.4a	8 851.0b		0.45a	
MC0	3 996.2a	9 305.2a		0.43b	
		2019	2020	2019	2020
D1	3 414.1c	7 170.3c	7 084.1c	0.47a	0.49a
D2	4 080.7b	8 772.3b	9 406.9b	0.46a	0.44b
D3	4 380.1a	10 561.8a	11 473.1a	0.41b	0.39c

Means within a column followed by different letters are significantly different at $P = 0.05$. MC: mepiquat chloride; MC0: no MC application; MC1: MC application; D1: 2.25 plants· m^{-2}; D2: 4.5 plants·m^{-2}; D3: 6.75 plants·m^{-2}

the minimum values. MC1D3 enhanced the seed cotton yield, and biological yield by 6.5% ~ 38.3%, and 1.9% ~ 65.8% compared with other combinations across both years, respectively.

*P*n and SPAD value

The *P*n and SPAD value at the EF and FB stages were significantly affected by year and MC application (Supplementary Table S2). The PPD interaction with MC significantly affected the SPAD value, but not the *P*n. The PPD-by-year interaction effect was significant for the *P*n, but not the SPAD value. The MC application improved the SPAD value but reduced the *P*n at the EF and FB stages (Table 2). Among the six combinations of PPD and MC, MC1D3 exhibited the maximum SPAD value followed by MC1D2 irrespective of years and sampling stages. MC1D3 increased the SPAD value by 2.6% ~ 26.8% at the FF, and by 1.3% ~ 11.7% at the FB relative to others in both years, respectively. MC0D1 showed the highest *P*n, while MC1D2 had the lowest *P*n regardless of years and sampling stages.

Specific leaf weight

PPD and sampling time significantly affected SLW (Supplementary Table S3). Significant MC effects on the SLW were detected in 2019. The two-way or three-way interaction effects involved in sampling time were significant except for MC × sampling time in 2020. During the period of PS to FB, SLW was basally decreased with increasing PPD under either MC application or free, but the trend was reversed at the FBO (Fig. 1). At the FBO stage, MC0D3 and MC1D3 displayed higher SLW compared with other treatments but there was no significant difference between MC0D3 and MC1D3. The SLW at the FBO was 56.9 $g \cdot m^{-2}$ for MC0D3 and 57.1 $g \cdot m^{-2}$ for MC1D3 in 2019, and 47.7 $g \cdot m^{-2}$ for MC0D3 and 48.9 $g \cdot m^{-2}$ for MC1D3 in 2020, respectively.

Table 2 The net photosynthesis rate (*P*n) and SPAD value in the main-stem functional leaves of upland cotton at the early flowering and flowering and boll setting in 2019 and 2020

Treatment	Early flowering				Flowering and boll setting		
	SPAD		*P*n /($\mu mol \cdot m^{-2} \cdot s^{-1}$)		SPAD	*P*n /($\mu mol \cdot m^{-2} \cdot s^{-1}$)	
	2019	2020				2019	2020
MC1D1	48.38c	47.31c	27.74c		50.91b	26.73d	30.57c
MC1D2	50.37b	48.76b	25.91e		52.45a	25.23e	27.40d
MC1D3	52.10a	49.57a	26.70d		53.14a	26.04de	28.44d
MC0D1	40.58f	39.62f	30.06a		50.10b	31.98a	34.15a
MC0D2	41.20e	40.57e	28.22bc		47.57c	29.89b	30.85bc
MC0D3	42.63d	41.79d	28.85b		47.31c	28.45c	32.21b
	2019	2020					
MC1	50.28a	48.54a	26.78b		52.17a	27.4b	
MC0	41.49b	40.66b	29.04a		48.33b	31.26a	
			2019	2020		2019	2020
D1	43.97a		27.35a	30.46a	50.50a	29.35a	32.36a
D2	45.24a		26.64a	27.49b	50.01a	27.56a	29.13b
D3	46.52a		26.27a	29.28a	50.23a	27.25a	30.33ab

Means within a column followed by different letters are significantly different at $P = 0.05$. MC: mepiquat chloride; MC0: no MC application; MC1: MC application; D1: 2.25 plants·m^{-2}; D2: 4.5 plants·m^{-2}; D3: 6.75 plants ·m^{-2}

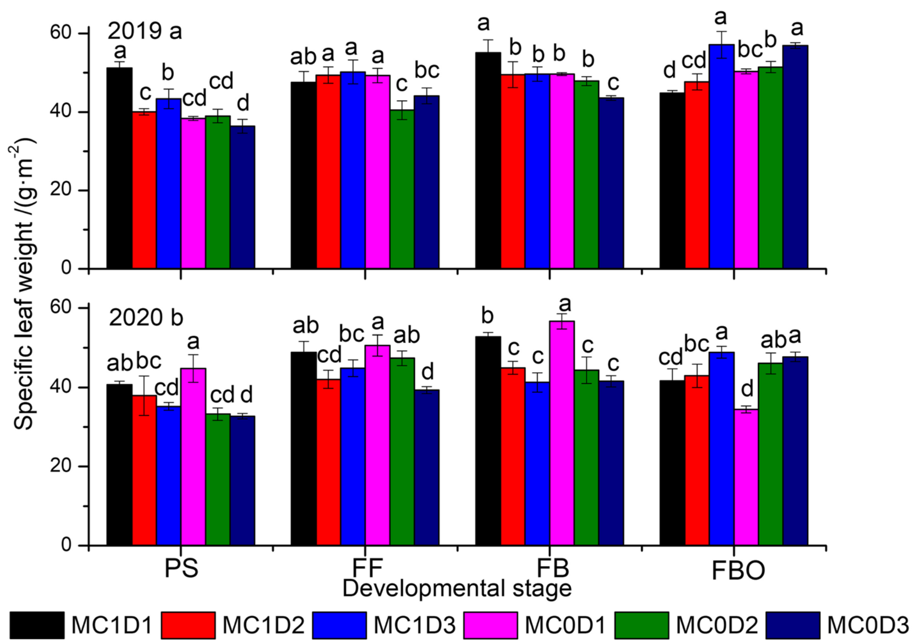

Fig. 1 Dynamics of specific leaf weight (**a**, **b**) as function of developmental stage in 2019 and 2020, respectively. Each data point represents the mean ± SD (n = 3). Within the same panel, means not sharing a common letter indicate significant differences at P < 0.05. PS: peak squaring; FF: first flowering; FB: flowering and boll setting; FBO: first boll opening; MC0: no mepiquat chloride application; MC1: mepiquat chloride application; D1: plant density of 2.25 plants·m^{-2}; D2: plant density of 4.5 plants·m^{-2}; D3: plant density of 6.75 plants·m^{-2}. The same as below

Chlorophyll concentration

MC, PPD, sampling time, and MC × PPD interaction significantly affected the Chl a, Chl b, and Chl a + b concentration except PPD effect on Chl a + b in 2019 (Supplementary Table S4). Each of the Chl a, Chl b, and Chl a + b showed a single-peak curve with a peak at the FB stage (Figs. 2 and 3). At that stage, MC1D3 exhibited the maximum in the three parameters followed by MC1D1 in 2019, while MC1D1 ranked first followed by MC1D3 in 2020. MC1D3 increased the Chl a by 0.5%, Chl b by 7.3%, and Chl a + b by 4.0% in 2019 (Fig. 2), but decreased the Chl a by 5.8%, Chl b by 1.3%, and Chl a + b by 4.4% in 2020 compared with MC1D1 (Fig. 3). Furthermore, MC application-improved Chl concentration pooled across three PPD levels was observed during the whole sampling period in both years (Supplementary Table S4, Figs. 2 and 3).

Nonstructural carbohydrate concentration

MC, PPD, and sampling time significantly affected the sucrose, hexose, starch, and TNC concentration except the PPD effects on the hexose concentration in 2020 (Supplementary Table S5). Significant two-way interaction effects of MC and sampling time, as well as PPD and sampling time, and three-way interaction effects of MC, PPD, and sampling time were detected for all parameters except the MC × sampling time interaction on the sucrose concentration in 2020. Each of the carbohydrate components (hexose, sucrose, and starch) and TNC concentration expressed similar trend, which was characterized by a rapid increase from the PS to FF and then a sharp decline until the FBO (Figs. 4 and 5). The maximum appeared at the FF and the minimum at the FBO regardless of treatment, carbohydrate type, and year. MC1D3 exhibited higher starch and TNC concentration compared with others at the FF stage. The starch concentration was elevated by 5.4% ~ 88.4% in 2019, and by 14.6% ~ 55.9% in 2020 in MC1D3 than in other treatments. The TNC concentration was increased by 7.8% ~ 52.0% in 2019, and by 13.5% ~ 39.7% in 2020 in MC1D3 relative to others. Averaged across three PPD levels, The starch concentration at the FF stage was increased by 42.5% in 2019 (P = 0.047), and by 38.0% (P = 0.012) in 2020 by the MC application. Likewise, the MC application improved the TNC concentration averaged across three PPD levels by 21.6% in 2019 (P = 0.069), and by 25.4% in 2020 (P = 0.023) compared with the MC-free control at the FF stage.

Carbohydrate metabolism enzyme activity

MC, PPD, and sampling time significantly affected the activities of SPS, SuSy, Rubisco, and FBPase except the PPD effect on the SuSy activity in 2019, and the MC effect on the Rubisco activity in 2020, respectively (Supplementary Table S6). The MC by PPD interaction effects

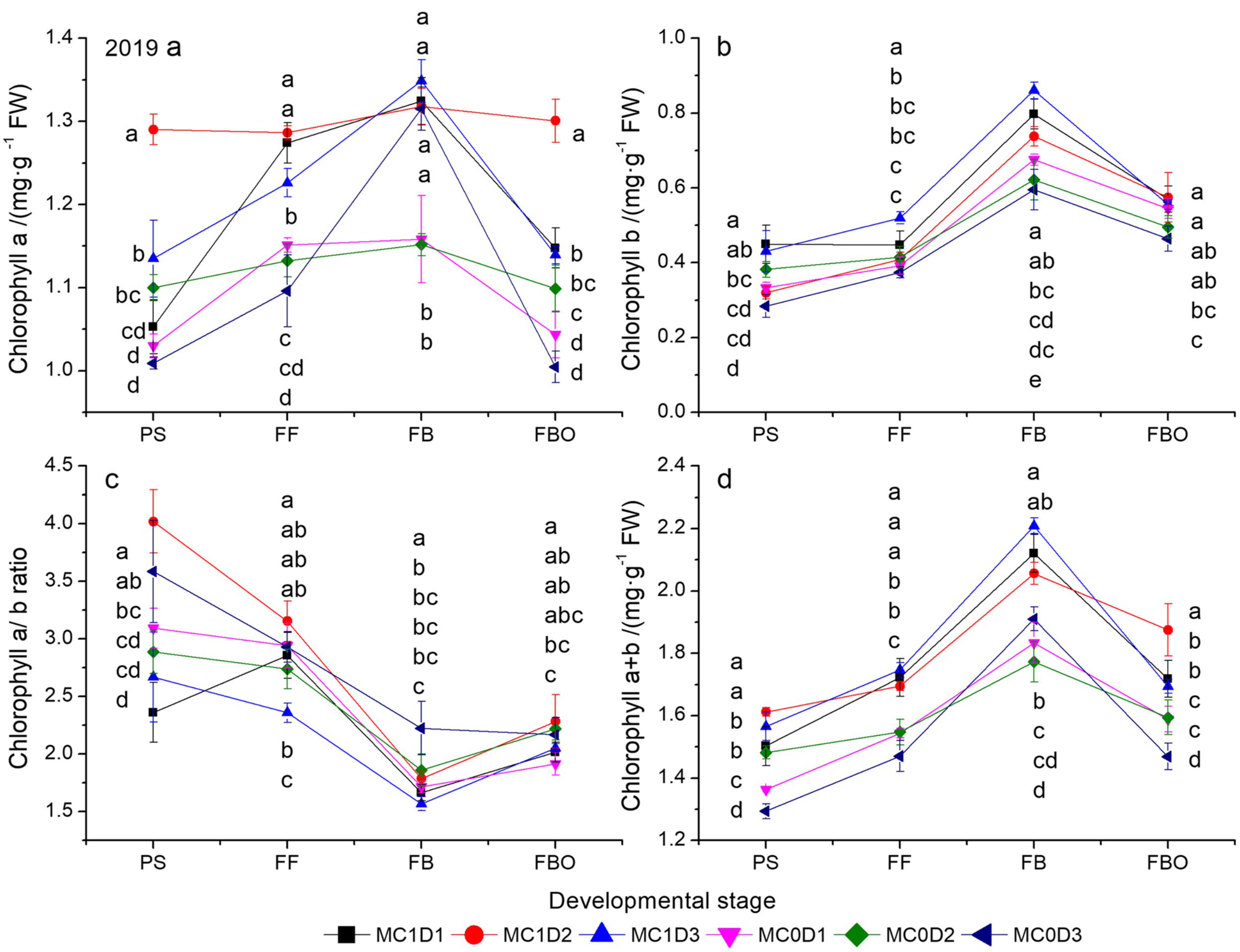

Fig.2 Changes of chlorophyll a (**a**), chlorophyll b (**b**), chlorophyll a/b (**c**), and chlorophyll a + b (**d**) concentrations as functions of developmental stage in 2019. Each data point represents the mean ± SD ($n=3$). At each sampling date, data points not sharing a common letter indicate significant differences at $P<0.05$

were significant for the activities of SPS, SuSy, Rubisco, and FBPase except for the SPS activity in 2020. The curve of Rubisco and FBPase activities showed a single-peak commonly at the FB stage (Figs. 6 and 7). The SuSy activity was typically increased up to the FF stage and then decreased down to the FBO stage. The SPS activity declined to the FB stage and then climbed up to the FBO stage. MC1D3 exhibited the maximal Rubisco activity at the FB stage in both years, which was 8.1% ~ 43.6% higher in 2019, and 2.5% ~ 53.2% higher in 2020 than those in other treatments (Figs. 6a, 7a). Moreover, MC1D3 continued to remain the maximal Rubisco activity at the subsequent FBO stage in 2020 (Fig. 7a). Nevertheless, the Rubisco activity averaged across three PPD levels in the MC treatment was reduced at the PS stage in 2019 ($P=0.024$) and the FF stage in 2020 ($P=0.040$), but was 17.2% and 28.1% higher than those in the MC free treatment at the FBO stage in 2019 and 2020, respectively. Averaged across three PPD levels, the FBPase activity was improved by the MC application at the FBO stage in both years ($P=0.017$ in 2019, $P=0.002$ in 2020). However, the MC application significantly reduced the FBPase activity at the PS stage ($P=0.029$) and FF stage ($P=0.007$) in 2020 (Figs. 6b, 7b). Similarly, the MC application significantly decreased the SPS activity at the FBO stage ($P=0.001$ in 2019, $P=0.053$ in 2020), and the SuSy activity at the FF stage ($P<0.001$ in 2019, $P=0.045$ in 2020).

Nonstructural carbohydrate transformation rate

Year, PPD, PPD × MC, and PPD × MC × year effects significantly affected the TRs of sucrose, hexose, starch, and TNC concentrations (Supplementary Table S7). MC application significantly affected the TRs of starch and TNC, but not the TRs of sucrose and hexose (Supplementary Table S7, Table 3). The middle PPD of 4.5 plants·m^{-2} had a lower TR of starch in 2019, and lower

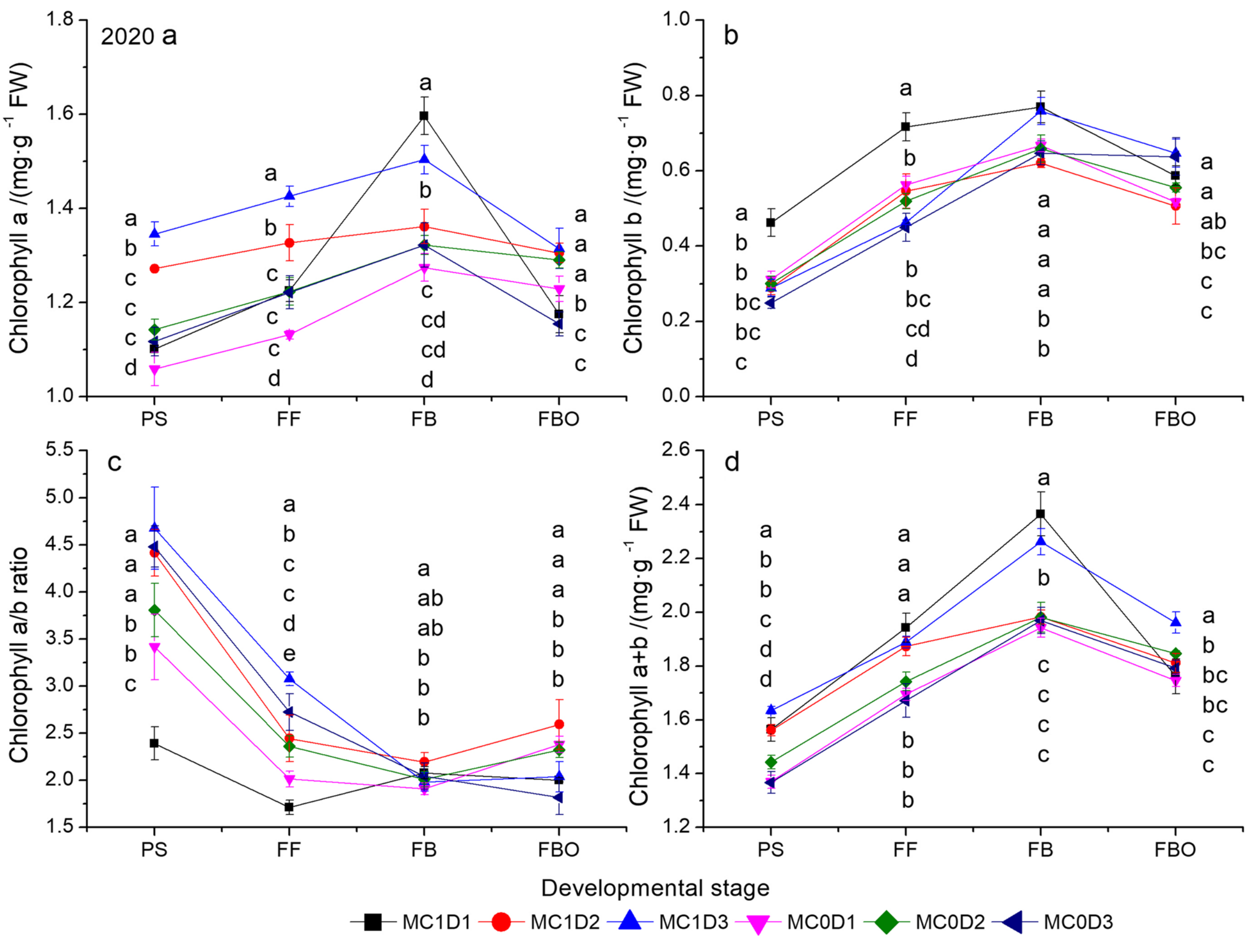

Fig. 3 Changes of chlorophyll a (**a**), chlorophyll b (**b**), chlorophyll a/b (**c**), and chlorophyll a + b (**d**) concentrations as functions of developmental stage in 2020. Each data point represents the mean ± SD (n = 3). At each sampling date, data points not sharing a common letter indicate significant differences at P < 0.05

TRs of TNC in both years compared with the lower and higher PPD levels (Table 4). The TRs of starch and TNC concentrations were increased by the MC application (Table 4). Among three combinations of MC application and PPD of three levels, MC1D3 exhibited a higher TR in starch than both of others in 2020 (Table 4). The TR of starch was increased by 15.3% ~ 52.7% in 2019, and by 9.8% ~ 11.1% in 2020 in MC1D3 than those in the three MC-free treatments.

Correlations between the Rubisco activity and the Chl concentration

A linear regression model was employed to fit the relationship between the Rubisco activity and multiple Chl concentration (Fig. 8). The regression fitting between the Rubisco activity and Chl a + b concentarion was better than that between the Rubico activity and Chl a concentration. Pooled across the period of the PS to FBO, the Rubisco activity was positively correlated with Chl a, Chl b, and Chl a + b concentration (Fig. 8).

Correlations between the nonstructural carbohydrate concentration and the carbon metabolism enzyme activity

The SuSy activity was positively correlated with the hexose, sucrose, starch, and TNC concentration in both years (Fig. 9). The correlations between SPS activity and the four nonstructural carbohydrate concentrations were significantly negative in 2020. The positive correlations between the Rubisco, and FBPase activities and sucrose, and hexose concentration were significant in 2020. There were highly significant and positive correlations between each two of those carbohydrate components and TNC in both years ($P \leq 0.001$). The SPS activity was negatively associated with the Rubisco and FBPase activities, while the latter two enzymes showed a significant and positive correlation in both years.

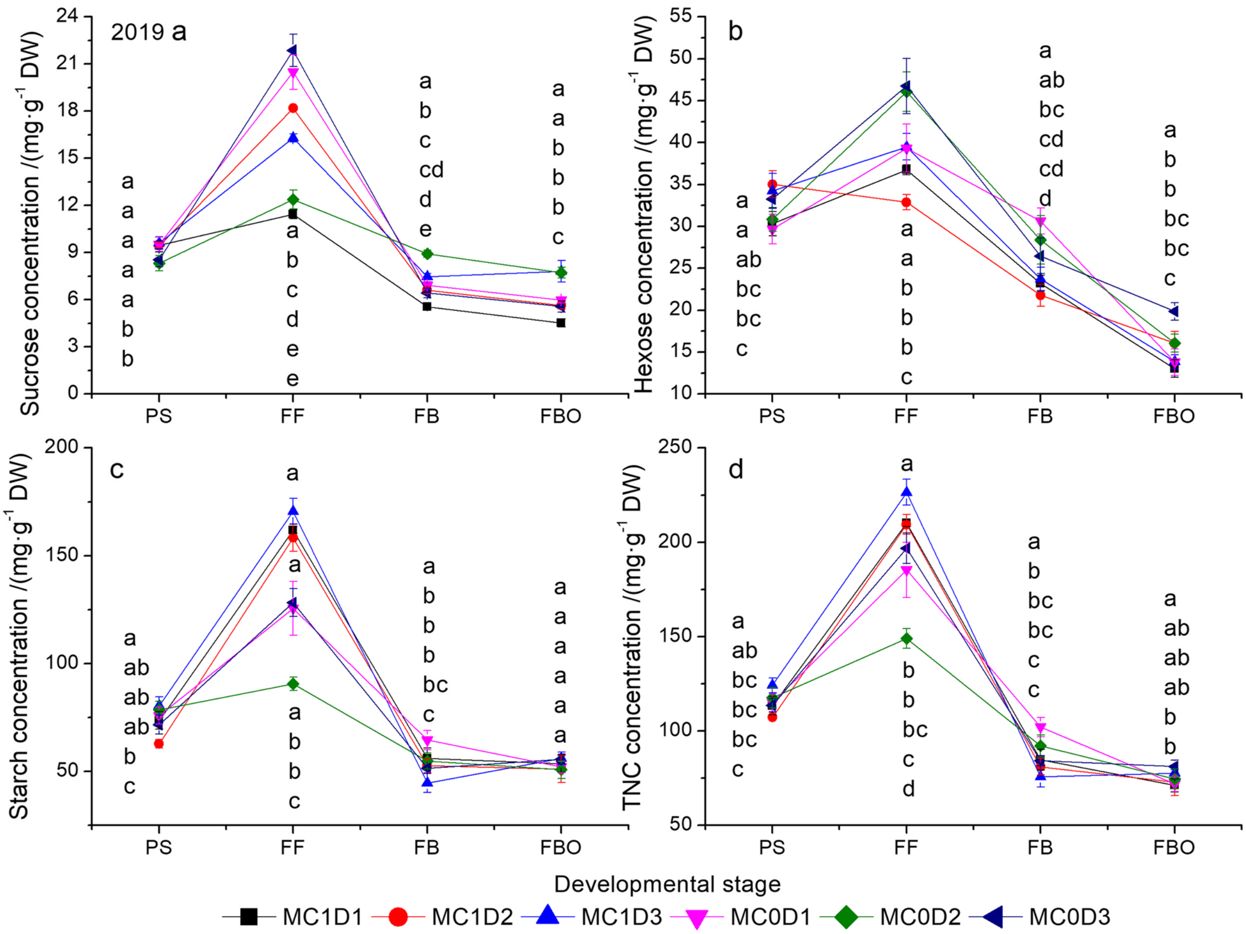

Fig. 4 Changes of sucrose (**a**), hexose (**b**), starch (**c**), and TNC (**d**) concentrations as functions of developmental stage in 2019. Each data point represents the mean ± SD ($n = 3$). At each sampling date, data points not sharing a common letter indicate significant differences at $P < 0.05$. TNC: total nonstructural carbohydrate. The same as below

Discussion

Increased PPD coupled with MC application improves seed cotton yield through the enhancement of the biological yield

Cotton lint yield is determined by either three yield components (boll density per unit land area, boll weight, and lint percentage) or dry matter accumulation and partitioning. In terms of the latter, the biological yield was increased, but the harvest index decreased as the PPD level increased (Table 1), which was supported by Dai et al. (2015) and Zhang et al. (2016). The MC application decreased the biological yield but increased the harvest index in both years, thus did not alter seed cotton yield (Table 1), which agrees with Cordeiro et al. (2021) who reported that MC application improved cotton harvest index. The plausible explanation for it is that MC supply prompts more biomass allocation to reproductive organs through the inhibition of vegetative ones. Among the six combinations of PPD of three levels and MC of two levels, MC1D3 had the greatest seed cotton yield, which was largely attributed to the highest biological yield (Table 1). Also, MC1D3 displayed a maximum in lint yiled resulted from a concurrent greatest boll sensity (Tang and Luo 2023; Luo and Tang 2023).

Increasing PPD coupled with MC application delays leaf senescence as indicated by higher SLW, Chl concentration, and Rubisco activity at the FB to FBO stage

The SLW was roughly decreased with increasing PPD levels before the FBO stage, but the trend was reversed at the FBO stage (Fig. 1a, b). At that time, MC1D3 exhibited the maximal SLW, being 0.3% higher in 2019, and 2.4% higher in 2020 than the second largest combination MC0D3. Pettigrew and Johnson (2005) reported an increased SLW by 4% due to MC application. Enhanced Chl concentration (either Chl a or Chl b) after

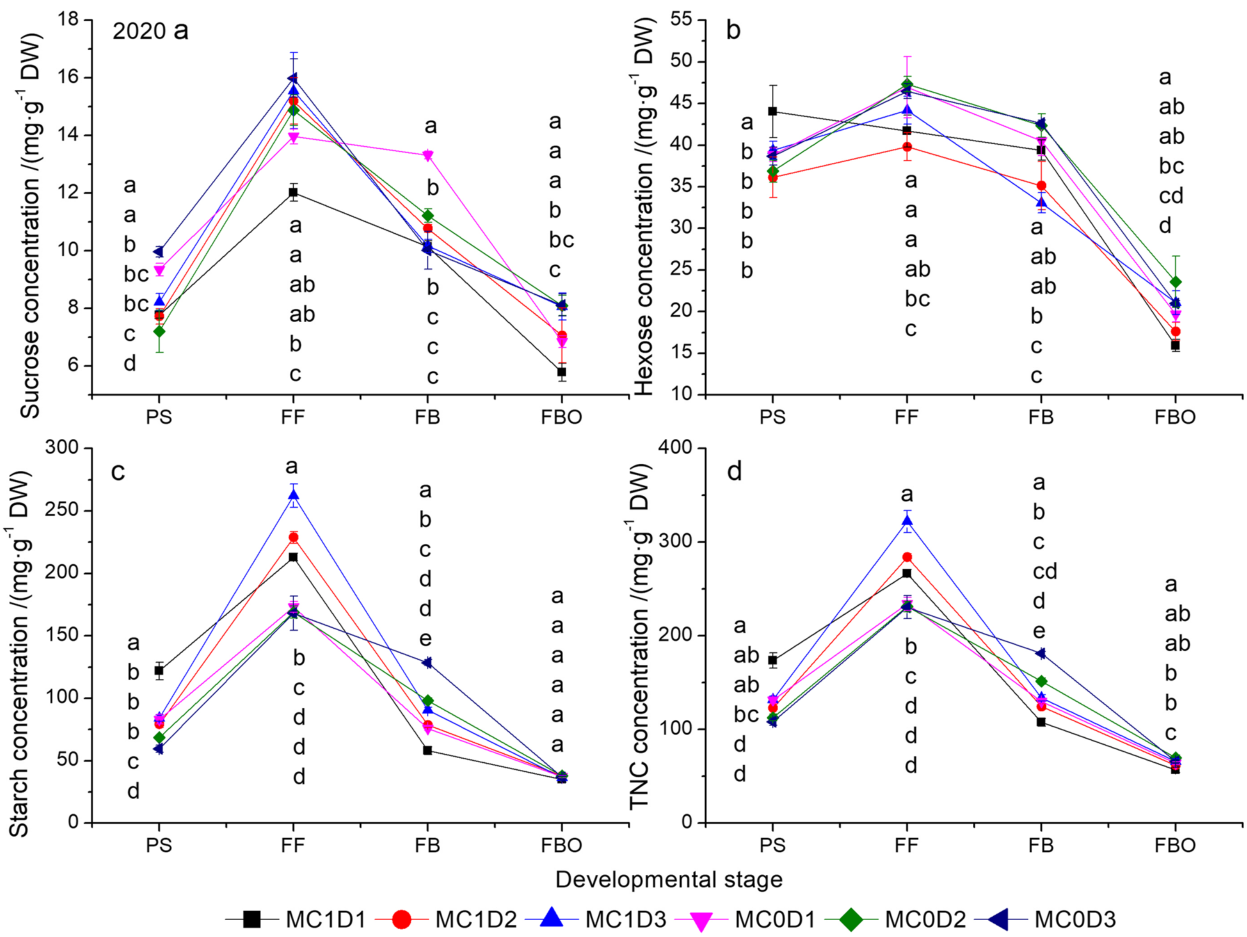

Fig. 5 Changes of sucrose (**a**), hexose (**b**), starch (**c**), and TNC (**d**) concentrations as functions of developmental stage in 2020. Each data point represents the mean ± SD ($n = 3$). At each sampling date, data points not sharing a common letter indicate significant differences at $P < 0.05$

cotton plants' exposure to MC application has been well recognized (Reddy et al. 1996; Tung et al. 2018a). The Chl a, Chl b, and Chl a + b concentrations pooled across all PPD levels were consistently higher during the PS to FBO stages in the MC application regime than in the MC free regime (Supplementary Table S4, Figs. 2 and 3). MC1D3 demonstrated the greatest Chl a, Chl b, and Chl a + b concentrations either at the FB stage in 2019 or at the FBO stage in 2020 (Figs. 2 and 3). Chlorophyll concentration is an important indicator of leaf senescence (Kong et al. 2016; Chen et al. 2018). Rubisco is a crucial rate-limiting enzyme responsible for CO_2 fixation in the Calvin cycle during photosynthesis. The Rubisco activity showed a rising trend through the PS to the FB and then declined sharply down to the FBO. MC1D3 exhibited the maximum Rubisco activity at the FB stage in 2019, and at the FB and FBO in 2020. The Rubisco activity was 2.6% ~ 53.2% higher at the FB stage in both years, and 2.4% ~ 52.7% higher at the FBO stage in 2020 than those in other treatments (Figs. 6a, 7a). MC application-decreased Rubisco activity was observed at the early reproductive stage as indicated by lower activity at the PS stage in 2019 ($P = 0.024$) and the FF stage in 2020 ($P = 0.040$). The result accords with the studies by Reddy et al. (1996) and Tung et al. (2019) where the activity of RuBP carboxylase was decreased in MC-treated plants. However, in the late reproductive stage such as the FBO, the MC application improved the Rubisco activity by 17.2% in 2019, and 28.1% in 2020. In addition, the positive correlations between the Rubisco activity and Chl a, Chl b, and Chl a + b were detected in both years (Fig. 8). Furthermore, delayed cotton leaf senescence due to increasing PPD has been observed (Dong et al. 2006, 2012; Luo et al. 2018). Taken together, MC1D3 was characterized by greater SLW, Chlorophyll concentration, and Rubisco activity at the late reproductive stage such as the FB and FBO stages, which should contribute to delayed leaf senescence together.

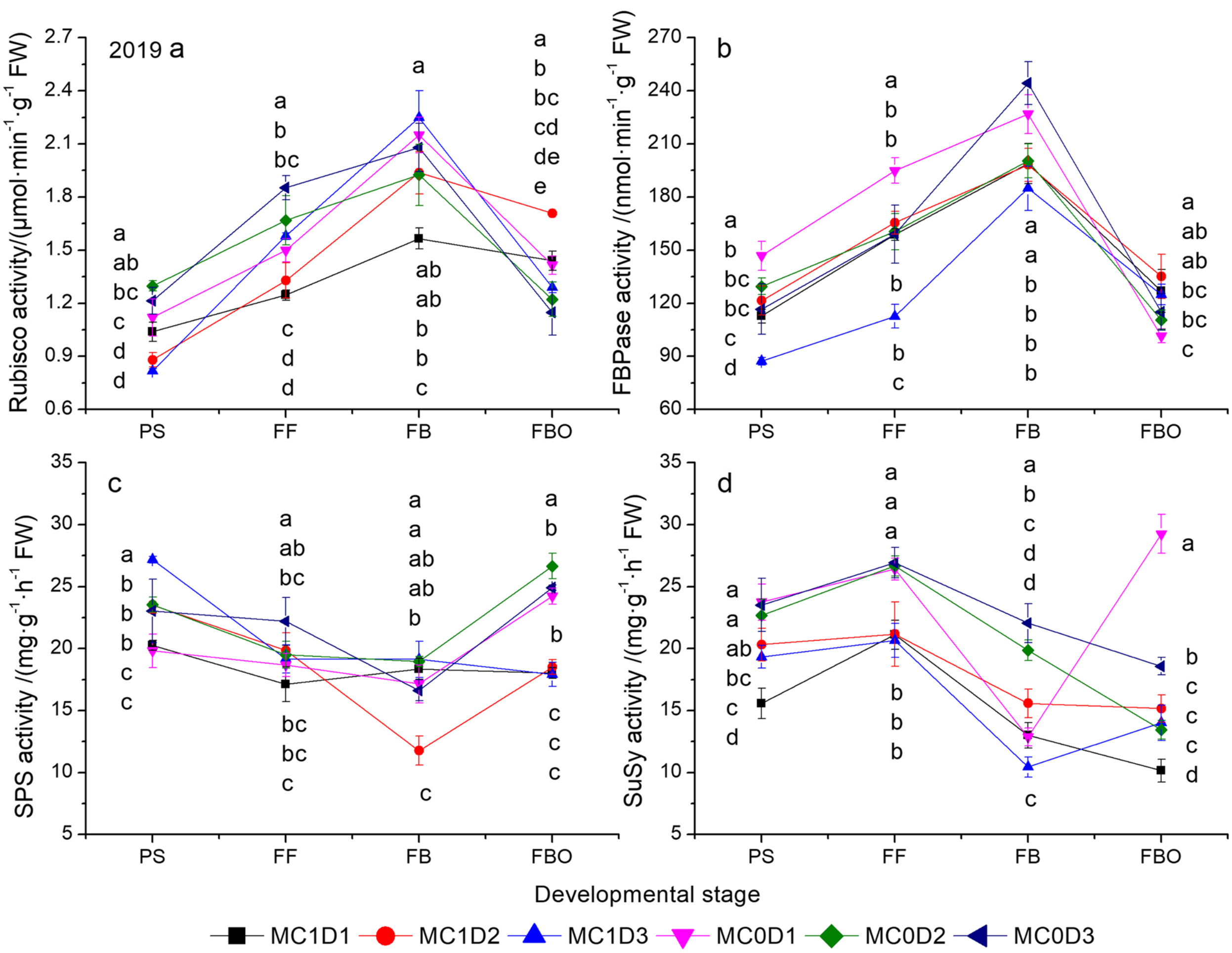

Fig. 6 Changes of Rubisco (**a**), FBPase (**b**), SPS (**c**), and SuSy activities as functions of developmental stage in 2019. Each data point represents the mean ± SD ($n=3$). At each sampling date, data points not sharing a common letter indicate significant differences at $P<0.05$. Rubisco: ribulose bisphosphate carboxylase oxygenase; FBPase: fructose-1, 6-bisphosphatase; SPS: sucrose phosphate synthase; SuSy: sucrose synthase. The same as below

Increasing PPD coupled with MC application enhances starch and TNC concentrations at early reproductive growth and their utilization efficiency

All carbohydrate components and TNC concentrations peaked at the FF stage and then declined at the FBO stage (Figs. 4 and 5). MC1D3 displayed higher starch and TNC concentrations at the FF stage, but no difference from or even lower than other treatments at the FBO stage over both years. Therefore, the greatest transformation rates of starch and TNC were produced in MC1D3 (Table 4). The higher starch concentration of MC1D3 at the FF is expected to result in a lower P_n at that time throught the feedback inhibition of photosynthesis (Table 2, Figs. 4c, 5c). On the other hand, the lower P_n may be also the result of the decreased Rubisco activity, as supported by the observations that they were synergistically decreased in MC-treated cotton leaves (Tung et al. 2018a, 2019; Reddy et al. 1996). We have also found that both P_n and Rubisco activity were reduced by MC application at the FF stage in both years (Table 2, Figs. 6a, 7a). An exceptional example comes from the report by Zhao and Oosterhuis (2000) who stated that MC application increased leaf CO_2 exchange rate. Notablely, above P_n was measured on a single leaf rather than on a whole canopy. Canopy gross photosynthesis was enhanced within 48 h after MC application (Hodges et al. 1991). MC1D3 is expected to enhance the canopy photosynthetic production on a population basis by increasing the population density as indicated by the first or second largest Leaf area index throught the whole reproductive growth phase (Tang and Luo 2023). Mao et al. (2014) found that increasing plant density significantly enhanced light use efficiency as mediated by improving light distribution in the cotton canopy. Moreover, the population photosynthetic production is potentially further elevated by the additional MC application, because the measure typically

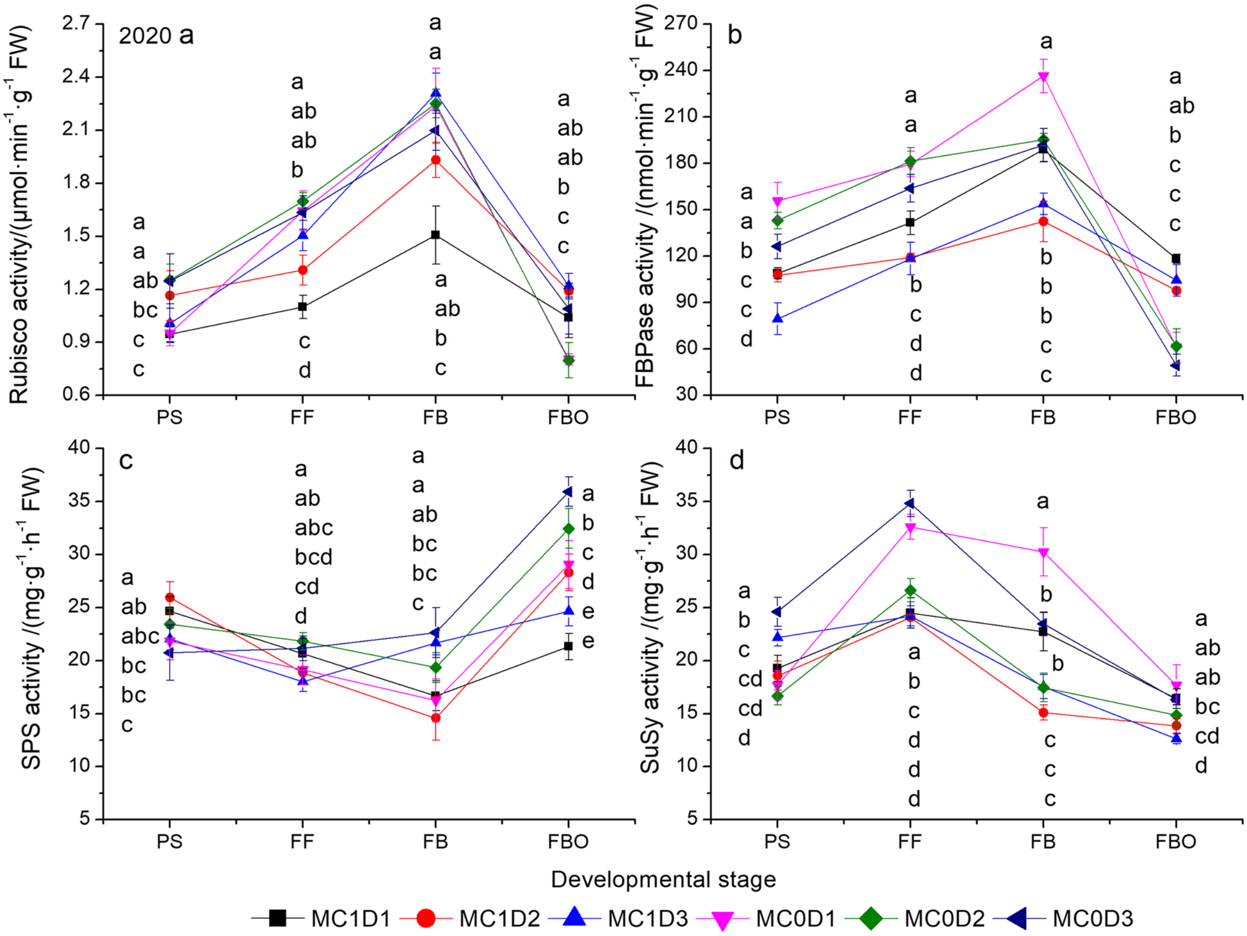

Fig. 7 Changes of Rubisco (**a**), FBPase (**b**), SPS (**c**), and SuSy activities as functions of developmental stage in 2020. Each data point represents the mean ± SD ($n = 3$). At each sampling date, data points not sharing a common letter indicate significant differences at $P < 0.05$

Table 3 The maximum, minimum, and transformation rate of sucrose and hexose concentrations in the main-stem functional leaves of upland cotton in 2019 and 2020

Treatment	Sucrose /(mg·g^{-1} DW)						Hexose /(mg·g^{-1} DW)					
	Max		Min		Rate		Max		Min		Rate	
	2019	2020	2019	2020	2019	2020	2019	2020	2019	2020	2019	2020
MC1D1	11.44e	12.02c	4.53c	5.78c	60.38b	51.89b	36.74b	41.69bc	13.03c	15.92d	64.51a	61.77a
MC1D2	18.19e	15.19ab	5.64b	6.37bc	69.00a	57.89a	32.86c	39.81c	16.05b	17.60 cd	51.20c	55.76abc
MC1D3	16.31d	15.56a	7.81a	8.07a	52.05c	47.99bc	39.50b	44.20ab	13.86ab	21.08ab	64.88a	52.32bc
MC0D1	20.48c	13.97b	5.99b	6.84b	70.72a	50.98bc	39.34b	46.96a	13.81ab	19.67bc	64.79a	57.91ab
MC0D2	12.38b	14.88ab	7.72a	8.10a	37.50d	45.51c	46.07a	47.33a	16.08b	23.58a	65.11a	50.10c
MC0D3	21.87a	15.99a	5.57b	8.12a	74.46a	49.20bc	46.75a	46.48a	19.85a	20.97ab	57.46b	54.87abc
MC1	15.31b	14.26a	5.99a	6.74b	60.47a	52.59a	36.37b	41.90b	14.32b	18.20b	60.20a	56.62a
MC0	18.24a	14.95a	6.43a	7.69a	60.89a	48.56b	44.05a	46.92a	16.58a	21.41a	62.45a	54.30a
D1	15.96b	13.00b	5.26b	6.31b	65.55a	51.43a	38.04b	44.33a	13.42b	17.80b	64.65a	59.84a
D2	15.29b	15.04a	6.68a	7.24a	53.25b	51.70a	39.47b	43.57a	16.07a	20.59a	58.16b	52.93b
D3	19.09a	15.78a	6.69a	8.09a	63.25a	48.60a	43.13a	45.34a	16.86a	21.03a	61.17ab	53.60b

Means within a column followed by different letters are significantly different at $P = 0.05$. MC: mepiquat chloride; MC0: no MC application; MC1: MC application; D1: 2.25 plants·m^{-2}; D2: 4.5 plants·m^{-2}; D3: 6.75 plants·m^{-2}

Table 4 The maximum, minimum, and transformation rate of starch and total nonstructural carbohydrate (TNC) concentrations in the main-stem functional leaves of upland cotton in 2019 and 2020

Treatment	Starch /(mg·g^{-1} DW)							TNC /(mg·g^{-1} DW)					
	Max		Min		Rate			Max		Min		Rate	
	2019	2020	2019	2020	2019	2020		2019	2020	2019	2020	2019	2020
MC1D1	162.03a	212.91c	53.58a	35.10a	66.91a	83.51b	210.21b		266.62c	71.15b	56.80c	66.14a	78.70a
MC1D2	158.45a	228.80b	51.11a	37.81a	67.65a	83.46b	209.50b		283.80b	72.80ab	61.78b	65.20a	78.23a
MC1D3	170.78a	262.30a	56.09a	36.60a	67.09a	86.05a	226.59a		322.05a	77.76ab	65.75ab	65.64a	79.58a
MC0D1	125.67b	173.12d	52.09a	37.40a	58.20b	78.39c	185.49c		234.05d	71.88b	63.92b	61.03ab	72.66b
MC0D2	90.63c	168.99d	50.79a	38.13a	43.93c	77.43c	149.09d		231.20d	74.59ab	69.81a	49.95c	69.81c
MC0D3	128.32b	168.13d	55.75a	36.86a	56.52b	78.01c	196.94bc		230.61d	81.16a	65.96ab	58.79b	71.35bc
MC1	163.75a	234.67a	53.59a	36.50a	67.22a	84.34a	215.43a		290.82a	73.90a	61.44b	65.66a	78.84a
MC0	114.87b	170.08b	52.87a	37.46a	52.88b	77.94b	177.17b		231.95b	75.88a	66.56a	56.59b	71.27b
D1	143.85a	193.02b	52.84a	36.25a	62.56a	80.95a	197.85b		250.33b	71.52b	60.36b	63.59a	75.68a
D2	124.54b	198.90b	50.95a	37.97a	55.79b	80.45a	179.29c		257.50b	73.70b	65.79a	57.57b	74.02b
D3	149.55a	215.22a	55.92a	36.73a	61.81a	82.03a	211.76a		276.33a	79.46a	65.86a	62.22a	75.47a

Means within a column followed by different letters are significantly different at $P=0.05$. MC: mepiquat chloride; MC0: no MC application; MC1: MC application; D1: 2.25 plants·m^{-2}; D2: 4.5 plants·m^{-2}; D3: 6.75 plants·m^{-2}

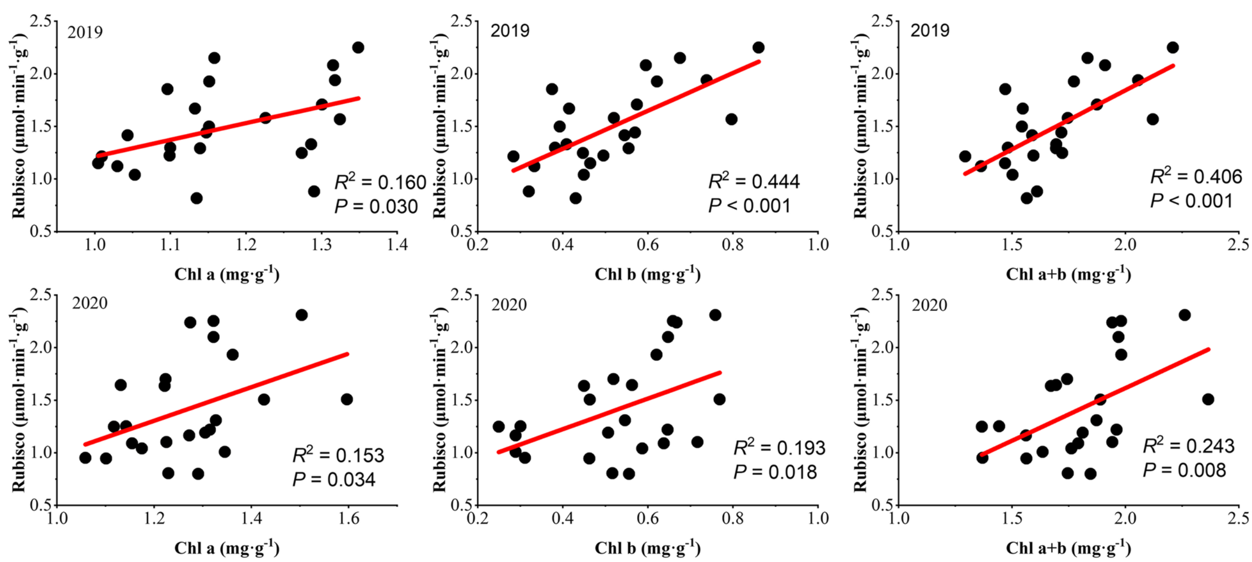

Fig. 8 Correlations between Rubisco activity and Chl a, Chl b, and Chl a + b concentrations in 2019 and 2020, respectively

inhibits leaf expansion, and creates compact plant stature, thus allowing more light penetration to the low-middle canopy. Gonias et al. (2012) reported that radiation use efficiency was significantly enhanced by 33.2% in MC application treatment, which was probably due to changes in leaf photosynthetic capacity and light configuration throughout the cotton canopy.

Starch is a predominant form of carbon reserves in plants. High starch and TNC concentration at the FF stage (early reproductive growth) in MC1D3 imply a higher carbon supply potential that is required for heavy boll load, which accords with the previous observation of a higher boll density in MC1D3 relative to other treatments in both years (Tang and Luo 2023; Luo and Tang 2023). In addition, the increased starch content induced by MC application did not affect photoassimilate export from leaves to young bolls (Zhao and Oosterhuis 2000). The combination of higher PPD and MC application is prone

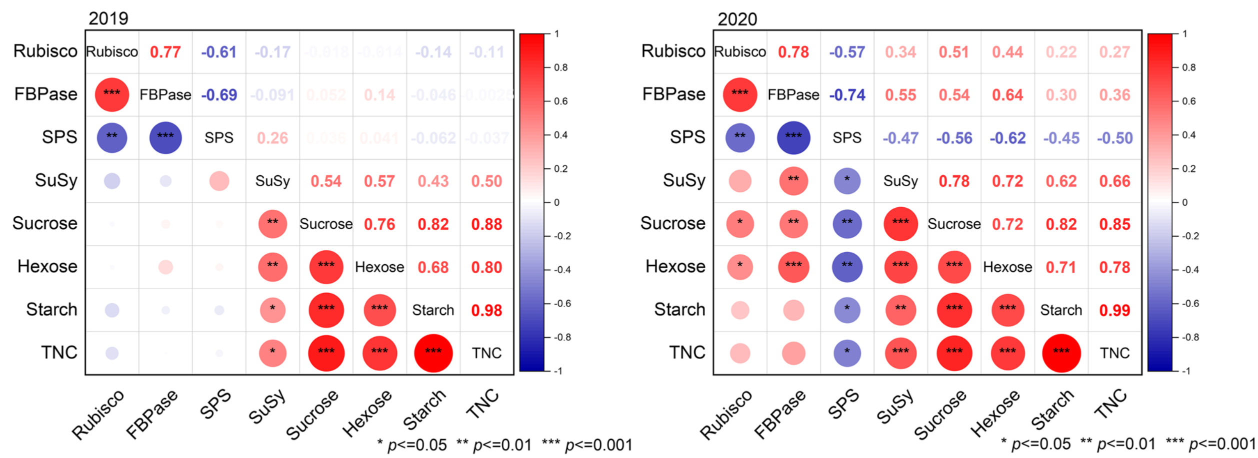

Fig. 9 Correlations between the activities of Rubisco, FBPase, SPS, and SuSy and the concentrations of hexose, sucrose, starch, and TNC in 2019 and 2020, respectively

to render boll setting more concentrated, increasing synchronous demand for photosynthate (Gwathmey and Clement 2010; Chen et al. 2021). The high transformation rate of starch throughout the FF to FBO stage in MC1D3 probably means a rapid starch degradation into soluble sugars for translocating into developing bolls, which help to synchronize boll maturation.

Conclusions

PPD of three levels (D1: 2.25 plants·m^{-2}, D2: 4.5 plants·m^{-2}, and D3: 6.75 plants·m^{-2}) and MC dosage of two levels (MC0: 0 g·ha^{-2}, MC1: 82.5 g·ha^{-2}) were combined to create six treatments. Among them, the highest PPD of 6.75 plants·m^{-2} combined with MC application (MC1D3) exhibited the highest seed cotton yield and biological yield. The sucrose, hexose, starch, and TNC concentration peaked at the FF stage and then declined to a minimum at the FBO stage. MC1D3 exhibited higher starch and TNC concentration compared with others at the FF stage. Since the concentration of starch and TNC at the FBO stage were either equal to or lower in MC1D3 than those in others, higher TRs were produced based on the interval of the FF to FBO stages. The high carbohydrate concentration and utilization efficiency in cotton leaves manifest a potential large source capacity with MC1D3. Higher SLW, Chlorophyll concentration, and Rubisco activity at the late reproductive stage help MC1D3 with delaying leaf senescence together. It is suggested that increasing PPD coupled with MC application improves cotton yield by enhancing leaf carbohydrate production and utilization efficiency and delaying leaf senescence.

Supplementary Information

The online version contains supplementary material available at https://doi.org/10.1186/s42397-023-00157-8.

Additional file 1: Supplementary Table S1. Mean squares from analysis of variance of the seed cotton yield, biological yield, and harvest index in 2019 and 2020. **Supplementary Table S2.** Mean squares from analysis of variance of the net photosynthetic rate (*Pn*) and SPAD value in the main-stem functional leaves of upland cotton at the early flowering (EF) and flowering and boll setting (FB) in 2019 and 2020. **Supplementary Table S3.** Mean squares from analysis of variance of specific leaf weight in 2019 and 2020. **Supplementary Table S4.** Mean squares from analysis of variance of the chlorophyll concentration in the main-stem functional leaves of upland cotton in 2019 and 2020. **Supplementary Table S5.** Mean squares from analysis of variance of the nonstructural carbohydrate concentration in the main-stem functional leaves of upland cotton in 2019 and 2020. **Supplementary Table S6.** Mean squares from analysis of variance of carbon metabolism-related enzyme activities in the main-stem functional leaves of upland cotton in 2019 and 2020. **Supplementary Table S7.** Mean squares from analysis of variance of the maximum, minimum, and transformation rate of nonstructural carbohydrate concentration in the main-stem functional leaves of upland cotton in 2019 and 2020.

Authors' contributions

Luo HL: Formal analysis; investigation; methodology; validation; visualization. Zhang ZX: Investigation; methodology; validation. Wu JF: investigation; methodology. Wu ZJ: Resources. Wen TW: Project administration; writing–review and editing. Tang FY: Conceptualization; data curation; formal analysis; funding acquisition; supervision; writing-original draft; writing–review and editing. All authors have read and agreed to the published version of the manuscript.

Funding

This work was supported by the National Natural Science Foundation of China (grant no. 31960385) and the Natural Science Foundation of Jiangxi, China (grant no. 20212BAB215009).

Availability of data and materials

The data presented in this study are available on request from corresponding author.

Declarations

Ethics approval and consent to participate
Not applicable.

Consent for publication
Not applicable.

Competing interests
The authors declare no conflict of interest.

Received: 27 July 2023 Accepted: 24 October 2023
Published online: 24 November 2023

References
Bednarz CW, Shurley WD, Anthony WS, et al. Yield, quality, and profitability of cotton produced at varying plant densities. Agron J. 2005;97:235–40. https://doi.org/10.2134/agronj2005.0235a.
Biles SP, Cothren JT. Flowering and yield response of cotton to application of mepiquat chloride and PGR-IV. Crop Sci. 2001;41:1834–7. https://doi.org/10.2135/cropsci2001.1834.
Cathey GW, Meredith WR. Cotton response to planting date and mepiquat chloride. Agron J. 1988;80:463–6. https://doi.org/10.2134/agronj1988.00021962008000030014x.
Chen Y, Kong X, Dong H. Removal of early fruiting branches impacts leaf senescence and yield by altering the sink/source ratio of field-grown cotton. Field Crop Res. 2018;216:10–21. https://doi.org/10.1016/j.fcr.2017.11.002.
Chen G, Luo H, Gao X, et al. Effects of late planting on fiber quality and within-boll yield components as mediated by sucrose metabolism in cotton bolls. Arch Agron Soil Sci. 2020;66:1319–33. https://doi.org/10.1080/03650340.2019.1666210.
Chen Y, Liu Z, Heng L, et al. Effects of plant density and mepiquat chloride application on cotton boll setting in wheat–cotton double cropping system. J Integr Agr. 2021;20:2372–81. https://doi.org/10.1016/S2095-3119(20)63286-5.
Cordeiro CF, Santos IF, Mello PR, et al. Cotton root growth response to mepiquat chloride application in early reproductive stages are cultivar dependent. Crop Sci. 2021;61:1987–95. https://doi.org/10.1002/csc2.20478.
Dai J, Li W, Tang W, et al. Manipulation of dry matter accumulation and partitioning with plant density in relation to yield stability of cotton under intensive management. Field Crop Res. 2015;180:207–15. https://doi.org/10.1016/j.fcr.2015.06.008.
Dong H. Major biological characteristics of cotton and their application in extensive high-yielding cultivation. China Cotton. 2013;40:1–3. (in Chinese).
Dong H, Li W, Tang W, et al. Yield, quality and leaf senescence of cotton grown at varying planting dates and plant densities in the Yellow River Valley of China. Field Crop Res. 2006;98:106–15. https://doi.org/10.1016/j.fcr.2005.12.008.
Dong H, Li W, Eneji AE, et al. Nitrogen rate and plant density effects on yield and late-season leaf senescence of cotton raised on a saline field. Field Crop Res. 2012;126:137–44. https://doi.org/10.1016/j.fcr.2011.10.005.
Galanopoulou-Sendouka S, Sficas AG, Fotiadis NA, et al. Effect of population density, planting date, and genotype on plant growth and development of cotton. Agron J. 1980;72:347–53. https://doi.org/10.2134/agronj1980.00021962007200020022x.
Gonias ED, Oosterhuis DM, Bibi AC. Cotton radiation use efficiency response to plant growth regulators. J Agr Sci. 2012;150:595–602. https://doi.org/10.1017/S0021859611000803.
Gu S, Evers JB, Zhang L, et al. Modelling the structural response of cotton plants to mepiquat chloride and population density. Ann Bot. 2014;114:877–87. https://doi.org/10.1093/aob/mct309%JAnnalsofBotany.
Gwathmey CO, Clement JD. Alteration of cotton source–sink relations with plant population density and mepiquat chloride. Field Crop Res. 2010;116:101–7. https://doi.org/10.1016/j.fcr.2009.11.019.
Hodges HF, Reddy VR, Reddy KR. Mepiquat chloride and temperature effects on photosynthesis and respiration of fruiting cotton. Crop Sci. 1991;31:1302–8. https://doi.org/10.2135/cropsci1991.0011183X003100050044x.
Khan A, Najeeb U, Wang L, et al. Planting density and sowing date strongly influence growth and lint yield of cotton crops. Field Crop Res. 2017;209:129–35. https://doi.org/10.1016/j.fcr.2017.04.019.
Kong X, Wang T, Li W, et al. Exogenous nitric oxide delays salt-induced leaf senescence in cotton (*Gossypium hirsutum* L.). Acta Physiol Plant. 2016;38:61. https://doi.org/10.1007/s11738-016-2079-9.
Li H. Principles and techniques of plant physiological biochemical experiment. Beijing: Higher Education Press; 2000.
Luo H, Tang F. Mepiquat chloride application combined with high plant population density promotes carbon remobilization in the roots of upland cotton. Plant Physiol Bioch. 2023;194:70–84. https://doi.org/10.1016/j.plaphy.2022.11.006.
Luo Z, Liu H, Li W, et al. Effects of reduced nitrogen rate on cotton yield and nitrogen use efficiency as mediated by application mode or plant density. Field Crop Res. 2018;218:150–7. https://doi.org/10.1016/j.fcr.2018.01.003.
Luo H, Chen G, Shao D, et al. Genotypic differences in sucrose metabolism with cotton bolls in relation to lint percentage. Field Crop Res. 2019;236:33–41. https://doi.org/10.1016/j.fcr.2019.03.012.
Mao L, Zhang L, Zhao X, et al. Crop growth, light utilization and yield of relay intercropped cotton as affected by plant density and a plant growth regulator. Field Crop Res. 2014;155:67–76. https://doi.org/10.1016/j.fcr.2013.09.021.
Mao L, Zhang L, Evers JB, et al. Yield components and quality of intercropped cotton in response to mepiquat chloride and plant density. Field Crop Res. 2015;179:63–71. https://doi.org/10.1016/j.fcr.2015.04.011.
Nichols SP, Snipes CE, Jones MA. Evaluation of row spacing and mepiquat chloride in cotton. J Cotton Sci. 2003;7:148–55.
O'Berry NB, Faircloth JC, Edmisten KL, et al. Plant population and planting date effects on cotton (*Gossypium hirsutum* L.) growth and yield. J Cotton Sci. 2008;12:178–87.
Owen Gwathmey C, Chism Craig C, Jr. Managing earliness in cotton with mepiquat-type growth regulators. Crop Manag. 2003;2:1–8. https://doi.org/10.1094/CM-2003-1222-01-RS.
Pettigrew WT, Johnson JT. Effects of different seeding rates and plant growth regulators on early-planted cotton. J Cotton Sci. 2005;9:189–98.
Rademacher W. Growth retardants: effects on gibberellin biosynthesis and other metabolic pathways. Ann Rev Plant Physiol Plant Mol Biol. 2000;51:501–31. https://doi.org/10.1146/annurev.arplant.51.1.501.
Reddy VR, Baker DN, Hodges HF. Temperature and mepiquat chloride effects on cotton canopy architecture. Agron J. 1990;82:190–5. https://doi.org/10.2134/agronj1990.00021962008200020004x.
Reddy VR, Trent A, Acock B. Mepiquat chloride and irrigation versus cotton growth and development. Agron J. 1992;84:930–3. https://doi.org/10.2134/agronj1992.00021962008400060004x.
Reddy KR, Boone ML, Reddy AR, et al. Developing and validating a model for a plant growth regulator. Agron J. 1995;87:1100–5. https://doi.org/10.2134/agronj1995.00021962008700060011x.
Reddy AR, Reddy KR, Hodges HF. Mepiquat chloride (PIX)-induced changes in photosynthesis and growth of cotton. Plant Growth Regul. 1996;20:179–83. https://doi.org/10.1007/BF00043305.
Ren X, Zhang L, Du M, et al. Managing mepiquat chloride and plant density for optimal yield and quality of cotton. Field Crop Res. 2013;149:1–10. https://doi.org/10.1016/j.fcr.2013.04.014.
Shah AN, Yang G, Tanveer M, et al. Leaf gas exchange, source–sink relationship, and growth response of cotton to the interactive effects of nitrogen rate and planting density. Acta Physiol Plant. 2017;39:119. https://doi.org/10.1007/s11738-017-2402-0.
Shi F, Li N, Khan A, et al. DPC can inhibit cotton apical dominance and increase seed yield by affecting apical part structure and hormone content. Field Crop Res. 2022;282:108509. https://doi.org/10.1016/j.fcr.2022.108509.
Shu H, Zhou Z, Xu N, et al. Sucrose metabolism in cotton (*Gossypium hirsutum* L.) fibre under low temperature during fibre development. Eur J Agron. 2009;31:61–8. https://doi.org/10.1016/j.eja.2009.03.004.
Siebert JD, Stewart AM. Influence of plant density on cotton response to mepiquat chloride application. Agron J. 2006;98:1634–9. https://doi.org/10.2134/agronj2006.0083.

Tang F, Luo H. Carbon remobilization in the stems of upland cotton as affected by mepiquat chloride and plant density. Field Crop Res. 2023;294:108864. https://doi.org/10.1016/j.fcr.2023.108864.
Tang F, Wang T, Zhu J. Carbohydrate profiles during cotton (*Gossypium hirsutum* L.) boll development and their relationships to boll characters. Field Crop Res. 2014;164:98–106. https://doi.org/10.1016/j.fcr.2014.06.002.
Tung SA, Huang Y, Ali S, et al. Mepiquat chloride application does not favor leaf photosynthesis and carbohydrate metabolism as well as lint yield in late-planted cotton at high plant density. Field Crop Res. 2018a;221:108–18. https://doi.org/10.1016/j.fcr.2018.02.027.
Tung SA, Huang Y, Hafeez A, et al. Mepiquat chloride effects on cotton yield and biomass accumulation under late sowing and high density. Field Crop Res. 2018b;215:59–65. https://doi.org/10.1016/j.fcr.2017.09.032.
Tung SA, Huang Y, Ali S, et al. Mepiquat chloride effects on potassium acquisition and functional leaf physiology as well as lint yield in highly dense late-sown cotton. Ind Crop Prod. 2019;129:142–55. https://doi.org/10.1016/j.indcrop.2018.11.056.
Wilson DG, York AC, Edmisten KL. Narrow-row cotton response to mepiquat chloride. J Cotton Sci. 2007;11:177–85.
Wrather JA, Phipps BJ, Stevens WE, et al. Cotton planting date and plant population effects on yield and fiber quality in the Mississippi Delta. J Cotton Sci. 2008;12:1–7.
York AC. Cotton cultivar response to mepiquat chloride. Agron J. 1983;75:663–7. https://doi.org/10.2134/agronj1983.00021962007500040020x.
Zhang D, Luo Z, Liu S, et al. Effects of deficit irrigation and plant density on the growth, yield and fiber quality of irrigated cotton. Field Crop Res. 2016;197:1–9. https://doi.org/10.1016/j.fcr.2016.06.003.
Zhao D, Oosterhuis DM. Pix plus and mepiquat chloride effects on physiology, growth, and yield of field-grown cotton. J Plant Growth Regul. 2000;19(4):415–22. https://doi.org/10.1007/s003440000018.
Zhao W, Du M, Xu D, et al. Interactions of single mepiquat chloride application at different growth stages with climate, cultivar, and plant population for cotton yield. Crop Sci. 2017;57(3):1713–24. https://doi.org/10.2135/cropsci2016.12.1008.